J Mater Sci: Mater Med (2008) 19:3515–3524
DOI 10.1007/s10856-008-3524-0

Periodontal regeneration in experimentally-induced alveolar bone dehiscence by an improved porous biphasic calcium phosphate ceramic in beagle dogs

Han Shi · Jia Ma · Ning Zhao · Yangxi Chen · Yunmao Liao

Received: 3 April 2008 / Accepted: 20 June 2008 / Published online: 15 July 2008

Abstract Regeneration of lost periodontium is the focus of periodontal therapy. To achieve the effective regeneration, a number of bone graft substitute materials have been developed. This study aimed to investigate the histological response in alveolar bone dehiscences which were filled with an improved biphasic calcium phosphate (BCP) ceramic with more reasonable pore diameter, pore wall thickness and porosity. Twenty-four alveolar bone dehiscences were made surgically in twelve beagle dogs by reflecting mucoperiosteal flaps on the buccal aspect of bilateral lower second premolars and removing alveolar bone. The left dehiscences were treated with BCP ceramic and the contralaterals were cured with the open flap debridement (OFD) as controls. Three dogs were used at week 4, 12, and 24 respectively. Histological observations were processed through three-dimensional micro-computed tomographic imaging, fluorescence and light microscopy. The histological study indicated that the biphasic ceramic was biocompatible, and regeneration was achieved more effectively through the BCP treatment. There were also arrest of epithelial migration apically and formation of new bone and cementum, as well as proliferation of fibrous connective tissues that became attached to the newly formed cementum at week 24, while there was no significant periodontal regeneration in the OFD group only with epithelial tissue migrating into the dehiscence regions. Clinically speaking, though the surgical location formed a limitation to the application of the improved BCP on the periodontal regeneration, the actual result was positive. It proved that the BCP had biocompatibility and was able to act as a stable scaffold to induce periodontal regeneration effectively.

Abbreviation

BCP	Biphasic calcium phosphate
μCT	Micro-computed tomography
CaP	Calcium phosphate
TCP	Tricalcium phosphate
β-TCP	β-Tricalcium phosphate
HA	Hydroxyapatite
PDL	Periodontal ligament
OFD	Open flap debridement

1 Introduction

The focus of periodontal therapy is always on the regeneration of lost periodontium. During common conditions, it appears that the epithelial tissues migrate rapidly into the wound, preventing periodontal regeneration [1, 2]. The tissue regeneration of the avascular and rigid side in the periodontal defect is a great problem. To achieve periodontal regeneration, various therapeutic procedures, including guided tissue regeneration (GTR), implantation of bone biomaterials and the application of various biologic mediators, either alone or in combination, have been developed [3–6].

H. Shi · N. Zhao · Y. Chen (✉) · Y. Liao
State Key Laboratory of Oral Diseases, Sichuan University, Chengdu, People's Republic of China
e-mail: cyxlfx@126.com
URL: http://www.editorialmanager.com/jmsm/default.asp

J. Ma
Department of Prosthodontics School of Stomatology, The Fourth Military Medical University, Xi'an, People's Republic of China

The use of some biomaterial as a barrier would ensure that the detached root surface became repopulated with cells from periodontal ligaments capable of forming bone, periodontal ligament and cementum. Many bone graft materials were available for helping to achieve a more predictable regeneration of osseous defects as well as the regeneration of all the periodontal attachment apparatuses around the teeth. It was thought that calcium phosphate (CaP) might stimulate osteogenesis at first and they had been used medically for bone regeneration [7]. However, when CaP was first used to treat bone defects, no positive result was obtained until Albee found that tricalcium phosphate (TCP) stimulated bone formation in the 1920s [8]. The use of CaP made a great progress in the field of material science between the 1970s and 1980s, and then it was extensively used for bone substitute in many clinical applications [9–12]. A series of calcium phosphate-based biomaterials including bioglass, glass ceramics, different calcium phosphate ceramics, cements, coatings and bioactive composites with calcium phosphates had been developed [13–18].

Among the wide variety of bone substitutes, researches had focused on biphasic calcium phosphate (BCP) ceramic, an outstanding bone graft composite material, which was made up of hydroxyapatite (HA) and β-tricalcium phosphate (β-TCP) with different proportions. Meanwhile, with applying nanometer technology in the field of biomaterials, some scholars [19–21] found porous nano-structure biomaterials as scaffolds for bone tissue engineering could greatly enhance the adhesion of materials, increase biodegradation and improve physical performance. However, porosity of the material was inversely proportional to the mechanical stability of BCP. That loss of stability was often cited as a limitation in the use of calcium phosphate-based ceramics in clinical practice. As for optimal regeneration, the degradation rate of bone graft substitute should equalize that of bone formation. By comparison, BCP, if composed of HA and β-TCP at the weight ratio of 40–60%, could have a higher degradation rate than HA solely and a better mechanical strength than β-TCP alone.

In this study, we treated the alveolar bone dehiscence with the BCP, observed the histological and morphological changes in the BCP group and the open flap debridement (OFD) control in the process of periodontal regeneration at week 4, 12 and 24 respectively, and evaluated the efficacy of the BCP.

2 Materials and methods

2.1 Biomaterial preparation

In this study, the BCP ceramic was made of hydroxyapatite (HA) and β-tricalcium phosphate (β-TCP) at the weight ratio of 40:60; grain size was controlled by changing the time and temperature of BCP precipitation; specifically, the BCP containing solution was stirred at room temperature for 24 h. Each BCP-containing solution was firstly centrifuged, filtered, and dried at 60°C for 8 h, then heated in air at 10°C/min from room temperature to a final temperature of 1,200°C, and sintered at this temperature for 60 min. Finally BCP samples were cut to cube (Fig. 1a).

The improvement of BCP was primarily reflected in its high porosity, and its minimum pore size was almost to a nanometer scale in three-dimensional space. Scanning electron micrographs of the improved BCP revealed that the pore distribution of BCP ceramic was uniform, with micropores distributed widely in the wall of macropores. The diameter of the macropore was approximately 300–500 μm (original magnification: × 80, Fig. 1b), minimum micropore size was almost less than 100 nm (original magnification: × 80,000, Fig. 1c). Through micro-computed tomography (μCT 80, Scanco Medical AG, Basserdorf, Swiss) analysis, the BCP exhibited a reasonably homogenous structure with the volume porosity of 85%, mean pore diameter of 162 μm (range, 116–515 μm) (Fig. 1d) and pore wall thickness of 66 μm (range, 36–144 μm) (Fig. 1e). All the pores were intercommunicated, and the BCP microstructure features thus could fully guarantee the access of nutrients and ideally encourage angiogenesis and neovascularization into the defect region.

BCP samples were degreased, ultrasonically cleaned and sterilized in a steam autoclave at 120° for 30 min according to standard laboratory procedures.

2.2 Animal preparation

Twelve healthy adult male beagle dogs about 2 years old and 18.3 ± 1.6 kg weight were enrolled in this study. They were supplied by the Experimental Animal Centre of Sichuan University (Chengdu, China). The study protocol was approved by the Animal Ethical Committee for Animal Research of Sichuan University (Chengdu, China). During the experiment, animals had free access to feed and water, and got accustomed with the environment 1 week prior to the operation.

2.3 Surgical procedure

Animals were anesthetized by intravenous injection of pentobarbital (pentobarbital, shanghai, China; 30 mg/kg). After shaving and disinfection preparation, 24 dehiscences were to be produced on the buccal aspect of bilateral lower second premolars of the 12 beagle dogs. At first, a full-thickness, mucoperiosteal flap was reflected and elevated to expose the buccal aspect of lower second premolars (P2), and then a rectangular piece of the buccal alveolar bone, 3 mm wide and 5 mm long, and deep

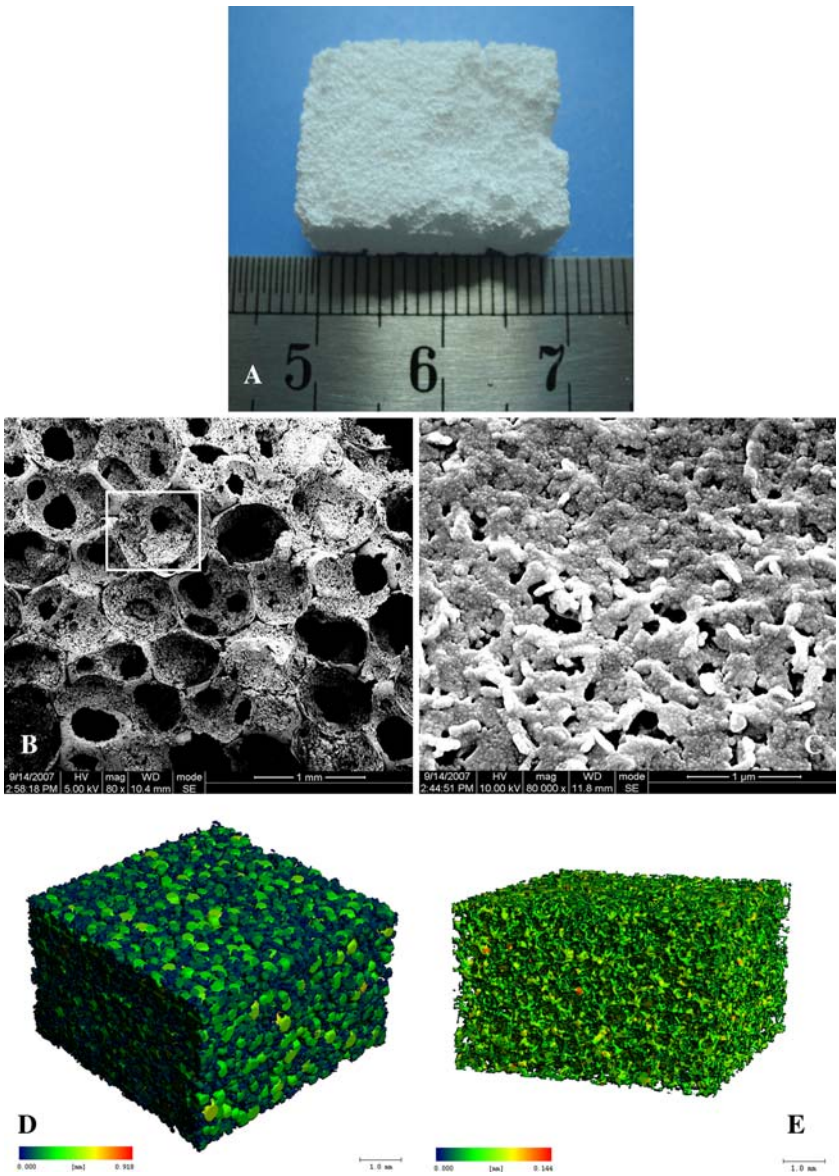

Fig. 1 Structural profile of the improved BCP. (**a**) The aspect of BCP sample; (**b**) BCP morphological observation by SEM (×80),Bar scales: 1 mm; (**c**) Magnified view of the white rectangle frame in (**b**) (×80,000) ,Bar scales: 1 μm; (**d**) 3D reconstruction image of BCP and pores by micro-CT, mean pore diameter of 162 μm. Bar scales: 1 mm; (**e**) Reconstruction image of BCP alone by micro-CT, mean pore wall thickness of 66 μm. Bar scales: 1 mm

enough to expose the root surfaces, was removed with a bone chisel (Fig. 2a). The dimension of the defect was verified with a periodontal probe (Williams periodontal probe, Hu-Friedy, Chicago, IL). A reference notch was made on the root surface at the bottom of the bone dehiscence. Defects were rinsed thoroughly with sterile saline. After BCP was immersed into the animal's blood, the left dehiscences were filled with BCP and the contralaterals were treated with OFD as controls. Finally, the flap was repositioned and sutured with Gore-Tex CV-5 suture (W.L. Gore & Associates, Flagstaff, AZ; Fig. 2b), and periodontal dressing placed to protect the wound and promote tissue healing (Fig. 2c). Postoperative antibiotic treatment was conducted twice daily for 3 consecutive days with 30,000 IU of penicillin G and 6 mg of gentamycin per kilogram of body weight. Plaque control was maintained throughout the experimental period by topical application of 0.2% solution of chlorhexidine gluconate spray (Hibitane concentrate, Sumitomo, Osaka, Japan) three times a week. The sutures were removed 2 weeks after the operation. The animals were allowed to ambulate freely after analepsia and received a liquid diet during the entire experimental period. At the end of experiment they were sacrificed with an overdose of sodium pentobarbital (pentobarbital, shanghai, China) through the cephalic veins. Three dogs were used at week 4, 12 and 24 respectively. Block sections of the teeth including alveolar bone and soft tissue were removed and fixed for 48 h in 4% paraformaldehyde solution, and then were dehydrated in a graded ethanol series.

Fig. 2 (**a**) Surgical procedures on the buccal aspect of lower second premolars. The chiseled bone block area in size of 5 × 3 mm^2, and deep to the root surface; (**b**) Defect treatment with BCP or OFD, then repositioning and suturing of the flap; (**c**) Periodontal dressing on the wound

2.4 Fluorescence labeling

The animals received polychrome sequence fluorescence labeling according to the following scheme: Oxytetracycline (Sigma-Aldrich, Munich, Germany), 20 mg/kg body weight, intravenous, post-operation immediately; Calcein Green (Sigma-Aldrich, Munich, Germany), 16 mg/kg body weight, intravenous, 4 weeks post-operation; Xylenol Orange (Sigma-Aldrich, Munich, Germany), 34 mg/kg body weight, intravenous, and 12 weeks post-operation [22].

2.5 Three-dimensional micro-computed tomography (μCT) analysis

The samples of three randomly selected dogs were firstly trimmed to proper size for the analysis chamber of the μCT device (μCT 80, Scanco Medical AG, Basserdorf, Swiss), then were mounted on a turntable that could be shifted automatically in the axial direction. Six hundred projections were taken over 180° or 360° of object rotation. The X-ray shadow projections were digitized as 1024 × 1024 pixels with 4096 brightness gradations (12 bit) for cooled camera or 256 gradations (8 bit) [23]. The spatial resolution obtained was 10 μm.

2.6 Histological examination

The samples were embedded in polymethylmethacrylate as separate blocks using Technovit 7200 (Heraeus–Kulzer, Wehrheim, Germany) without decalcification. The blocks were trimmed firstly to proper cross section using a circular diamond saw (Leica SP 1600, Germany). Then 6 sections of 5 μm thickness and another 6 sections of 10 μm were cut from each sample along the buccal-lingual direction and parallel to the long axis of the teeth with a microtome (Leica SM 2500E, Germany).

Serial sections of 5 μm were stained with Hematoxylin and Eosin (H&E) staining and examined under light microscope. The 10 μm sections without staining were observed by a fluorescence microscope (Olympus IX71, Tokyo, Japan). High resolution, low magnification of 4, digital fluorescent micrographs were made through transmission light (DAPI-, FITC- and rhodamine-type filter sets for Oxytetracycline, Calcein Green and Xylenol Orange fluorescence, respectively), and then combined with digital image acquisition. The images of the histological sections were captured by a digital camera connected to that light microscope with a magnification of 100.

3 Results

3.1 Surgeries

All surgeries went well and clinical healing in both groups was uneventful without significant inflammation in all defects after operation. No adverse reactions, such as material exposure, toxic signs, or suppuration, were observed throughout the experimental period.

3.2 Three-dimensional micro-CT (μCT) analysis

3.2.1 Qualitative analysis

μCT evaluation guaranteed clear differentiation between teeth and bone tissues using a global thresholding procedure[24], where a threshold over 265 was used to be identified as bone tissues, whereas that below 265 teeth. The reference notch at the buccal aspect of P2 root surface was visible in the reconstructed 3D images of teeth alone (Fig. 3a); while it became invisible in the reconstructed 3D images of the teeth together with its surrounding alveolar bone of BCP groups (Fig. 3f, h). This showed that the defect region had new bone formation and the notch had been covered by newly formed bone. However, the reconstructed images of OFD controls, regardless of the week 4 or the week 24 group, revealed the reference notch clearly, meaning that no new bone formation had occurred. (Fig. 3b, d).

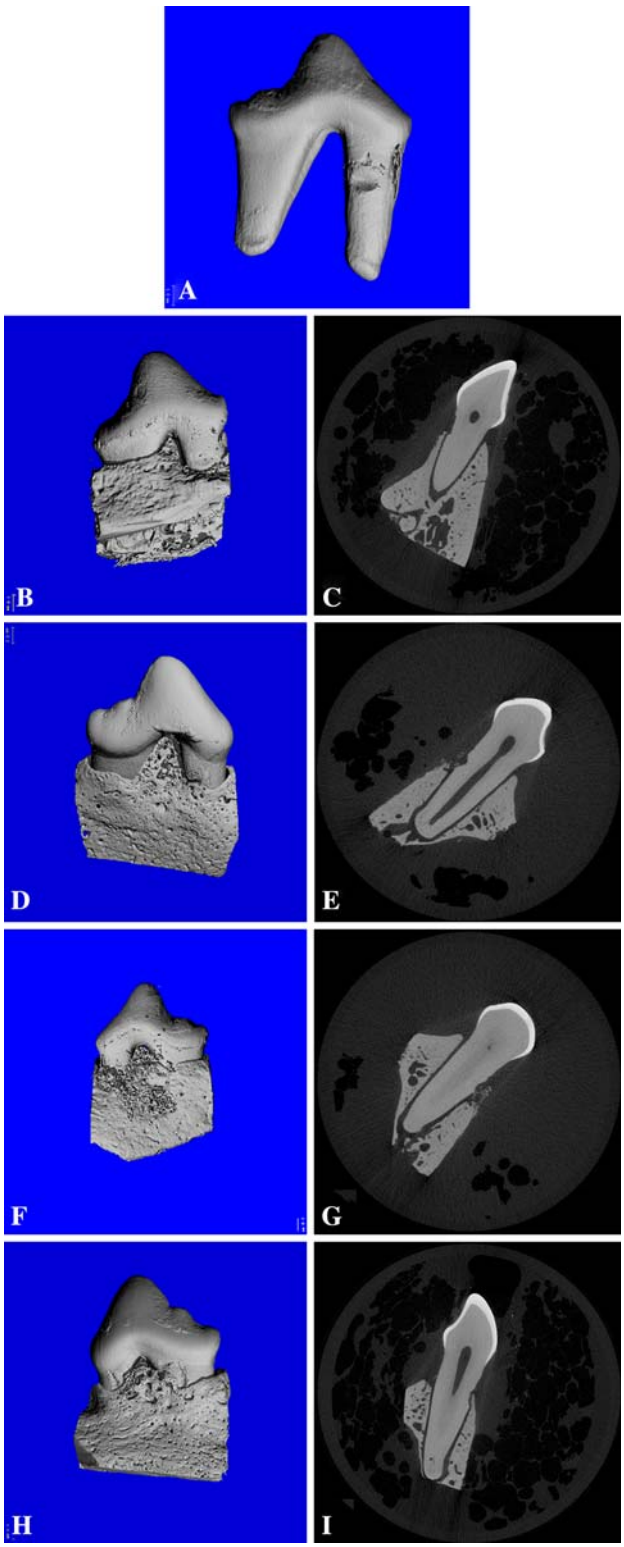

◀ **Fig. 3** Images of reconstructed sample and single slice. (**a**) Reconstructed 3D images of teeth alone showed the reference notch made by the bone chisel; (**b**) Reconstructed images of OFD at week 4, could reveal the reference notch clearly without any bone formation; (**c**) Slice image of (**b**); (**d**) Reconstructed images of OFD at week 24; (**e**) Slice image of (**d**); (**f**) Reconstruction image of BCP at week 4, and the defect was filled with bone matrix and materials which had not fully degraded yet; (**g**) Slice image of (**f**), tissue density of the defect region was obviously lower than the surrounding normal bone tissue; (**h**) Reconstruction image of BCP at week 24, the new bone was close to its original height; (**i**) Slice image of (**h**), tissue density of defect region was also near to the normal bone

At the week 4 BCP group, the 3D reconstruction images of BCP groups displayed that the defect region was filled with the mixture of bone matrix and material which had not fully degraded yet. Its surface was rough and uneven, similar to the scaffold material, but showed significant difference with the neighbor bone tissues (Fig. 3f).

At the week 24 BCP group, the defect region had obvious new bone formation and the bone had regenerated to or close to its original height (Fig. 3h, i).

3.2.2 Quantitative analysis

The morphometric parameters were determined from the micro-tomographic data sets using direct 3D morphometry [25, 26]. Through selecting the same volume of host bone and newly formed bone in the experimental groups and calculating with triangulation (TRI) method, the differences between them were found (Table 1). With the extension of experimental period, the degree of maturity of the new bone was also increased and approximated to host bone all the more.

3.3 Fluorescence microscopy

Fluorescence labeling was applied to visualize newly formed bone tissues. And sequential fluorochrome labels revealed the dynamics of bone formation. Fluorochrome deposited together with calcium in the bone formation process. Oxytetracycline was injected at the initial stage of reparation. The deposition was invisible possibly because the flurochrome had been metabolized out of the body or new bone had not formed yet. Calcein Green and Xylenol Orange were present in the healing bone of the transverse process and marked the areas of bone tissue regeneration in order. At the 24th week of BCP group, the formation of new bone was apparent, and the main labeling lines of the newly-formed bone ranked in parallel. The line of Calcein Green showed light green at medial bone (Fig. 4a), and the line of Xylenol Orange displayed light yellow at lateral bone (Fig. 4b). The area between the two lines of light yellow and light green was the new bone (Fig. 4c), and the two marker-lines showed the deposition of bone mineralization. In OFD group, no bone formation could be seen but a notch on the root surface and migratory epithelium (Fig. 4d).

3.4 Histological analysis

Histological analysis revealed no signs of acute inflammation or foreign body giant cell reaction in any samples. In the BCP sites, the formation of new bone was apparent.

Table 1 Quantitative results about newly formed bone of experimental group (TRI)

	BV (mm^3)	TV (mm^3)	BV/TV (%)	Tb.N (1/mm)	Tb.Th (μm)	Mean density (mg HA/ccm)
4w	0.0208	0.0861	24.09	0.3122	0.0956	332.14 ± 149.53
12w	0.0481	0.0866	55.54	2.4073	0.1601	660.92 ± 150.36
24w	0.0718	0.0891	80.21	3.2661	0.2685	795.83 ± 154.59
HB	0.0798	0.0859	93.46	3.9468	0.2793	975.88 ± 149.53

Note: BV: new bone volume; TV: total volume; BV/TV: relative bone volume; Tb.N: trabecular number; Tb.Th: trabecular thickness; HB: host bone(as control)

μCT scanning was progressed at 4, 12 and 24 weeks after implantation

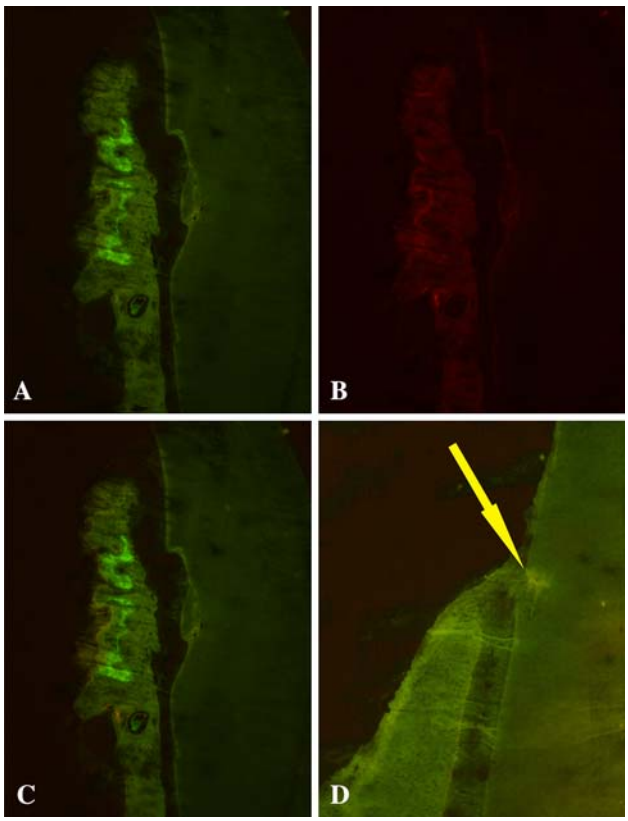

Fig. 4 (**a**) At the 24th week of BCP, Calcein Green showed light green in the inner bone; (**b**) At the 24th week of BCP, Xylenol Orange displayed light yellow at the outer bone; (**c**) Composition of (**a**) and (**b**), the area between the two lines of light yellow and light green was the new bone formed from 4 to 24 weeks; (**d**) No bone formation could be seen and only epithelial tissue migration on the notch (yellow arrow) at the 24th week of OFD

Four weeks after operation: (1) OFD: defect region was filled with granulation tissues together with abundant leukomonocytes and white cells. The capillaries diffused widely, and fiber-like tissues alignment was rambling (Fig. 5a, b); (2) BCP: close observation of bone formation showed that abundant blood vessels and osteoid tissues secreted by osteoblast-like cells were growing into the material. The large number of pores, found in the newly-formed tissues, was the undegradable BCP (Fig. 6a, b).

Twelve weeks after operation: (1) OFD: inflammatory response disappeared, and a large disorderly array of fiber trabs inserted into the notch of root surface could be seen. The surface of notch had been covered by collagen and formed a renewable connection with the fibers (Fig. 5c, d). (2) BCP: clear osteoblast line, newly formed bone matrix, osteocytes, and mineralized bone were observed on the host bone bed. New cementum had deposited on the old cementum and root planed dentin. Fibroblasts and angiogenesis in periodontal ligament (PDL) grew actively (Fig. 6c, d).

Twenty-four weeks after operation: (1) OFD: the newly-formed bone near the notch were invisible, with only epithelium and connective tissue covering the notch for periodontal repair instead of regeneration (Fig. 5e, f); (2) BCP: new cementum was always formed on the root surface. The alveolar bone in the bone dehiscence was reformed and the PDL were reorganized. Collagen fibers were observed adjacent to the newly formed cementum, and most of them were inserted into cementum and adjacent bone at right angles (Fig. 6e, f).

4 Discussion

The regeneration of lost periodontium is always a great problem in clinical treatment, due to the anatomic structure of periodontium and cellular responses. The main anatomic challenge is poor vascular supply and micro-movement of the wound tissues due to masticatory forces [27]. At the cellular level, the epithelium migrates at a rate of 0.5 mm/day, considerably faster than the rate of migration of the PDL and bone-forming cells [28]. However, PDL cells are capable of migrating only a short distance, with or without placement of a physical barrier to exclude the epithelium and connective tissue [1, 2, 29]. The junctional epithelium covers the exposed root surface prior to the osteogenic fibroblasts and osteoblasts repopulating the wound site, and affects the periodontal regeneration directly [30–32].

Presumably, by allowing more time and space for only cells from bone tissues and PDL to repopulate in the dehiscence (that is a porous scaffold material as bone graft

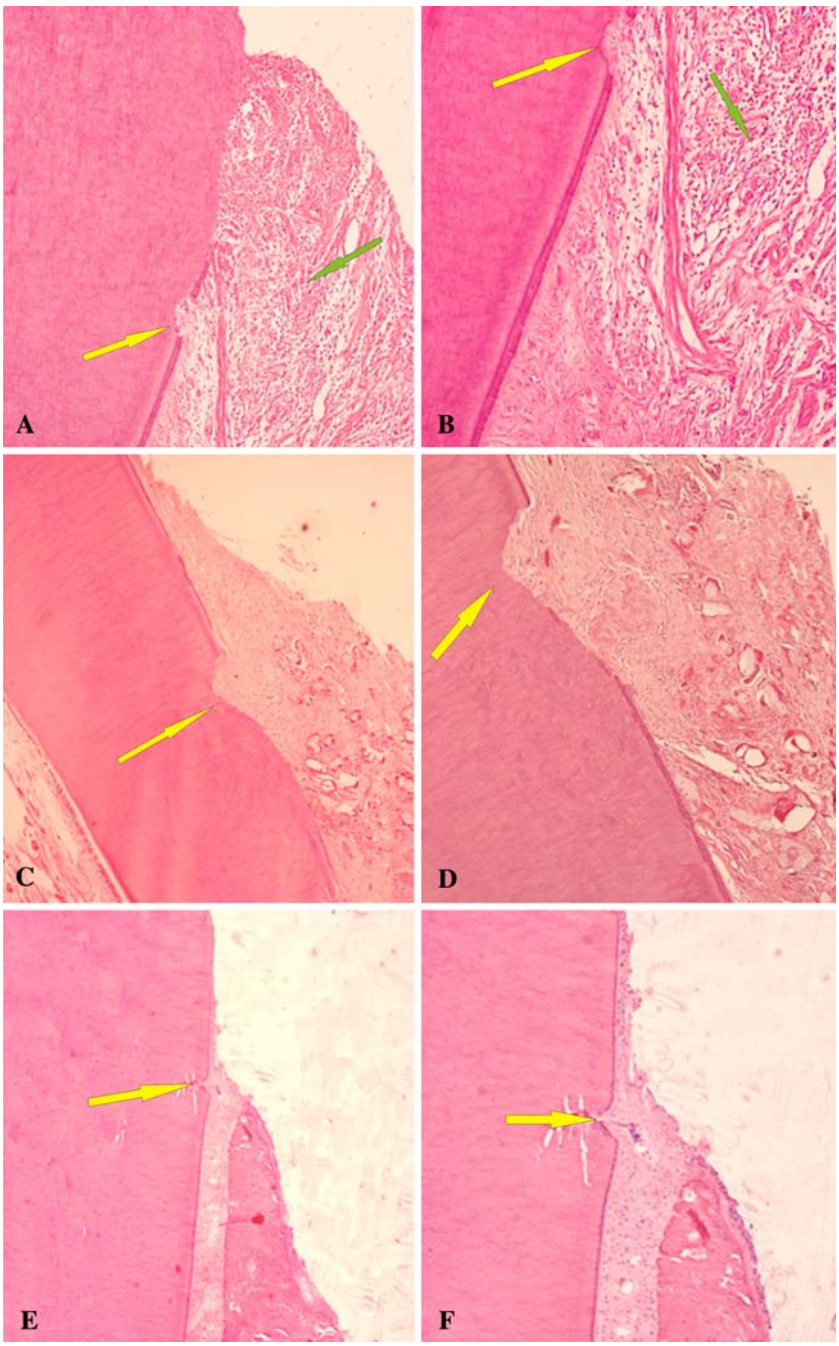

Fig. 5 Histological micrographs of periodontal repair in OFD controls at different time: (**a**) 4 weeks: inflammatory cell (green arrow) infiltrated in the defect (×40); (**b**) Magnified view of (**a**) (×100); (**c**) 12 weeks: a large disorderly array of fiber trabs inserted into the notch (yellow arrow) (×40); (**d**) Magnified view of (**c**) (×100); (**e**) 24 weeks: epithelium and connective tissue (green arrow) covered the notch (×40); (**f**) Magnified view of (**e**) (×100). Decalcified section stained with Hematoxylin and Eosine staining

placed into the area), periodontal regeneration is facilitated. That is why we always hope to utilize some biomaterials as a barrier to prevent epithelium from growing into the defects, and as a medium to facilitate new cementum, attachment apparatus and bone formation.

Between the 1920s and 1970s, some literatures reported that CaP was capable of osteoconduction and facilitating bone formation [33, 34]. The TCP used by Nery (it was subsequently identified by LeGeros in 1988) consisted of 20% β-TCP and 80% HA [35, 36]. This material and other mixtures of β-TCP and HA were later described as BCP. From then on, BCP ceramic had been studied as a bone graft substitute because of its close chemical and crystal resemblance to bone minerals. Extensive fundamental studies and clinical applications had also demonstrated that BCP was biocompatible and osteoconductive [9, 12, 37, 38]. All that evidence explained why we applied BCP as a bone graft substitute for periodontal regeneration.

Another factor for using BCP is its porosity. To induce bone formation effectively, the architectural properties of the ceramic are (1) the macropores are interconnected and big enough for soft tissues and blood vessels to grow

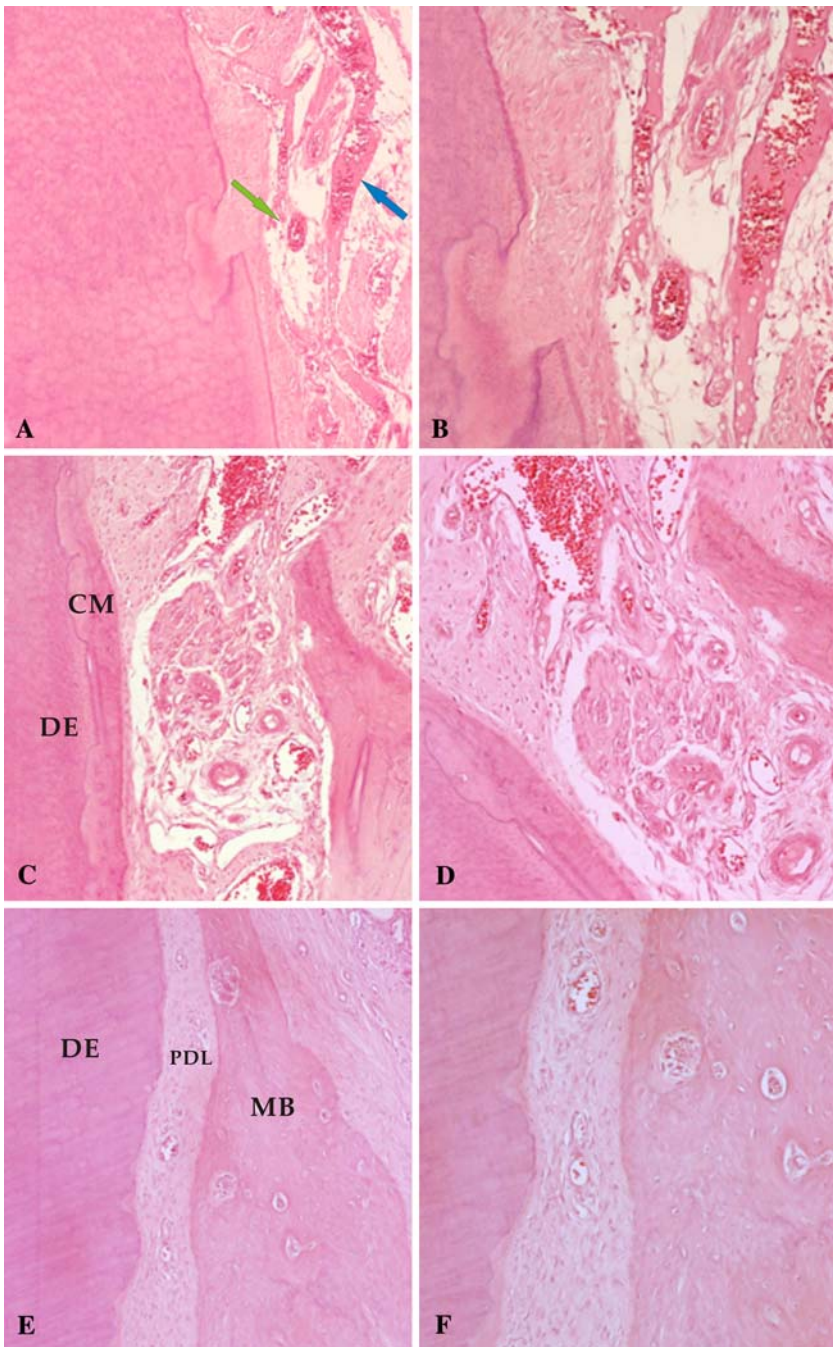

Fig. 6 Histological micrographs of periodontal regeneration in BCP experimental group. (**a**) 4 weeks: abundant blood vessels (green arrow) and osteoid tissues (blue arrow) grew into the materials (×100); (**b**) Magnified view of (**a**) (×200); (**c**) 12 weeks: new cementum (CM) had deposited on the root planed dentin (DE), fibroblasts and angiogenesis is in periodontal ligament grew actively, newly-formed bone matrix and osteocytes were observed on the host bone bed (×100); (**d**) Magnified view of (**c**) (×200); (**e**) 24 weeks: new cementum (CM) was always formed on the root surface, mature bone (MB) in bone dehiscence was clear and the periodontal ligament (PDL) were reorganized. Decalcified section stained with Hematoxylin and Eosine staining (×100); (**f**) Magnified view of (**e**) (×200). Decalcified section stained with Hematoxylin and Eosine staining

in; (2) the macropore surface has microporous structures [39–41]. Porosity can greatly increase the surface area of ceramic, facilitating greater degradation. Additionally, porosity may enable bone morphogenic proteins (BMP) to adsorb on material surface and reach greater local concentrations than the threshold value that needed to induce bone formation [34, 42, 43]. Porosity also can enhance the adhesion, proliferation and deposition of osteogenic cells. Reasonable pore sizes are responsible for better nutrient, cell distribution and capillary formation. The optimal pore size of the ceramic implants for osteoinduction is 150–500 μm. Pore sizes higher than 300 μm, however, are recommended to make room for the formation capillaries [44]. It is also notable that,with the porosity increasing, the graft will be significantly more brittle with lower compressive strength. High mechanical strength is an essential property for a bone substitute material.

After continuous research, a BCP made of HA and β-TCP at the weight ratio of 40:60 was obtained using a technique integrating the gel casting with polymer sponge methods [45]. We named it improved porous BCP ceramic. The so-called improved BCP mainly referred to the

improvement in its more reasonable pore diameter, pore wall thickness and porosity. The improved BCP had abundant micro pores that were distributed widely in the walls of the macro pores, with a mean pore diameter of 162 μm and porosity high up to 85%.

Material factors such as surface area affected the biological degradation, and in general, the larger the surface area, the greater the biodegradation. The porous structure of the BCP thus could promote the degradation rate greatly. Due to the resemblance of the BCP porosity and microstructure to human cancellous bone, incorporation of capillaries, perivascular tissue and osteoprogenitor cells into the material bed will be accelerated. Its network structure as physical barriers would promote guided tissue regeneration by physically inhibiting gingival epithelium and connective tissues and favor repopulation of the periodontal defect by cells from the periodontal ligament and alveolar bone preferably.

The improved BCP consisting of 40% HA and 60% β-TCP in weight ratio in this study, was an optimal compromise between degradation and mechanical strength. For regeneration to occur, cells capable of forming cementum, bone and PDL must occupy the periodontal defect and produce these specialized tissues. All these mean that the graft must stay in the defect until it is replaced by newly-formed periodontium, which also means that it should have a higher mechanical strength. In addition, BCP ceramic with a block form has been studied. Matthias et al. [46] have demonstrated that a block form is more efficient than the particular form and new bone apposition happens with progressive material degradation.

Wound stabilization may be yet another critical mechanism to promote periodontal regeneration besides material property. There is growing evidence that wound stabilization may be a critical variable in the early stages of periodontal wound healing to achieve periodontal regeneration**.** When a periodontal flap is replaced in OFD, a blood clot is formed between the flap and the root surface. The fibrin of the clot forms the initial attachment to the root surface, preventing epithelial from covering and forming a scaffold for the development of a cell and collagen fiber attachment mechanism. This initial fibrin attachment to the root surface is easily disturbed and requires protection until the replacement by collagen fibrils occur. So is it also the case of BCP. Therefore, in order to avoid BCP running off and keep the wounds of both groups from loading forces until collagen fibrils and bone matrix ingrowths occurred, the wound areas of animals were covered with periodontal dressing and animals were fed on liquid diet during the entire experimental period. These would contribute to wound stabilization.

Some literatures [47–49] reported that an 8-week healing interval has been required to evaluate periodontal repair in dogs. Choi et al. [50] also introduced that no differences in bone morphogenetic protein were noted between an 8- and 24-week intervals, that is, an 8-week healing period is sufficient to observe the initial healing process. However, the degradation of BCP and the formation of new periodontium were a long process. In order to observe the possible intact change of periodontal regeneration, we chose week 4, week 12, and week 24 as study points.

In addition, probing methods often got some "false" gains because of resolution of inflammation, bone fill, reformation of the gingival collagen fibers and a long junctional epithelium. They are therefore not adequate to evaluate periodontal regenerative therapies. Histological evaluation is the only reliable method of judging the efficacy of regenerative periodontal therapies. At the same time, we adopted μCT reconstruction to learn the visual change of alveolar bone formation.

The histological findings of OFD in this study were in accordance with previous studies [30–32]. The healing pattern of OFD group was characterized by extensive migration of junctional epithelium into the bone dehiscence region in the whole therapic period. Under high power lens, connective tissue fibers were aligned parallel to the root surface. The junctional epithelium covered the notch and migrated slightly apical to the coronal (Fig. 5e, f). The formation of new bone was invisible. In BCP, there was a clear process of cell attachment on BCP surface, cell and capillary proliferation and differentiation, bone matrix formation by osteoblast-like cells, and then mineralization of bone matrix to replace the BCP completely at last. Through μCT images (Fig. 3f–i), we could get a more direct recognition of alveolar bone regeneration in BCP.

The volume of periodontal regeneration depended on many factors, such as material property, position of the defect, study period, and so on. The choice of surgical district will have a direct impact on the effectiveness of regeneration. The reason of district definition in our study is that buccal aspect dehiscence is the most common periodontium loss in our clinical treatment. Few literatures, however, reported the therapy on it. Though the volume of periodontal regeneration in this study was still far from being ideal, the efficacy of the BCP is positive.

As a candidate for periodontal regeneration, the improved BCP is cohesive in application, rigid sufficiently to maintain the space during the healing period, osteoconductive, and biodegradable. It works as a scaffold to provide space for periodontal tissue formation, and as a barrier to obstruct epithelium invading quickly into the territory of alveolar bone and PDL. In addition, it might eventually be proved to be a suitable carrier of various growth factors for tissue engineering.

5 Conclusion

Through applying the BCP ceramic that improved the connectivity of pores and porosity of it in the alveolar dehiscence, the result confirmed the efficacy of the BCP for periodontal regeneration, and provided a favorable choice for practical bone graft substitute for periodontal therapy. However, this topic should be confirmed by further experimentation over a longer period of time. Moreover, its predictability in a clinical situation remains to be determined.

References

1. S. Nyman, J. Lindhe, T. Karring, H. Rylander, J. Clin. Periodontol. **9**, 290 (1982). doi:10.1111/j.1600-051X.1982.tb02095.x
2. J. Gottlow, S. Nyman, J. Lindhe et al., J. Clin. Periodontol. **13**, 604 (1986). doi:10.1111/j.1600-051X.1986.tb00854.x
3. M.A. Brunsvold, J.T. Mellonig, Periodontology 2000 **1**, 80 (1993). doi:10.1111/j.1600-0757.1993.tb00209.x
4. J. Murakami, T. Kato, S. Kawai, S. Akiyama, A. Amano, I. Morisaki, J. Periodontol. **79**, 721 (2008). doi:10.1902/jop.2008.070400
5. D.L. Cochran, J.M. Wozney, Periodontology 2000 **19**, 40 (1999). doi:10.1111/j.1600-0757.1999.tb00146.x
6. T. Karring, J. Lindhe, P. Cortellini, *Clinical Periodontology and Implant Dentistry* (Munksgaard, Copenhagen, 2003)
7. M. Jarcho, Clin. Orthop. Relat. Res. J. **157**, 259 (1981)
8. F.H. Albee, Ann. Surg. **71**, 32 (1920). doi:10.1097/00000658-192001000-00006
9. N. Passuti, G. Daculsi, J.M. Rogez, S. Martin, J.V. Bainvel, Clin. Orthop. Relat. Res. **248**, 169 (1989)
10. A.O. Ransford, T. Morley, M.A. Edgar et al., J. Bone Joint Surg. Br. **80**, 13 (1998). doi:10.1302/0301-620X.80B1.7276
11. R. Cavagna, G. Daculsi, J.M. Bouler, J. Long Term Eff. Med. Implant **9**, 403 (1999)
12. J. Delecrin, S. Takahashi, F. Gouin, N. Passuti, Spine **25**, 563 (2000). doi:10.1097/00007632-200003010-00006
13. K. de Groot, Biomaterials **1**, 47 (1980). doi:10.1016/0142-9612(80)90059-9
14. L.L. Hench, J. Wilson, Science **226**, 630 (1984). doi:10.1126/science.6093253
15. C.J. Damien, J.R. Parsons, J. Appl. Biomater. **2**, 187 (1991). doi:10.1002/jab.770020307
16. K. de Groot, R. Geesink, C.P. Klein, P. Serekian, J. Biomed. Mater. Res. **21**, 1375 (1987). doi:10.1002/jbm.820211203
17. A.A. Mirtchi, J. Lemaitre, N. Terao, Biomaterials **10**, 475 (1989). doi:10.1016/0142-9612(89)90089-6
18. P. Ducheyne, J.M. Cuckler, Clin. Orthop. Relat. Res. **276**, 102 (1992)
19. K.A. Hing, S.M. Best, W. Bonfield, J. Mater. Sci. Mater. Med. **10**, 135 (1999). doi:10.1023/A:1008929305897
20. J.F. De Oliveira, P.F. De Aguiar, A.M. Rossi et al., Artif. Organs **27**, 406 (2003). doi:10.1046/j.1525-1594.2003.07247.x
21. T.J. Webster, C. Ergun, R.H. Doremus, R.W. Siegel, R. Bizios, Biomaterials **22**, 1327 (2001). doi:10.1016/S0142-9612(00)00285-4
22. H.J. Erli, M. Ruger, C. Ragoss et al., Biomaterials **27**, 1270 (2006). doi:10.1016/j.biomaterials.2005.08.001
23. R. Cancedda, A. Cedola, A. Giuliani et al., Biomaterials **28**, 2505 (2007). doi:10.1016/j.biomaterials.2007.01.022
24. R. Muller, P. Ruegsegger, Stud. Health Technol. Inform. **40**, 61 (1997)
25. T. Hildebrand, A. Laib, R. Muller et al., J. Bone Miner. Res. **14**, 1167 (1999). doi:10.1359/jbmr.1999.14.7.1167
26. O. Gauthier, R. Muller, D. von Stechow et al., Biomaterials **26**, 5444 (2005). doi:10.1016/j.biomaterials.2005.01.072
27. U. Sakallioglu, G. Acikgoz, B. Ayas et al., Biomaterials **25**, 1831 (2004). doi:10.1016/S0142-9612(03)00468-X
28. S. Garrett, G. Bogle, Periodontology 2000 **1**, 100 (1993). doi:10.1111/j.1600-0757.1993.tb00211.x
29. J. Caton, S. Nyman, H. Zander, J. Clin. Periodontol. **7**, 224 (1980). doi:10.1111/j.1600-051X.1980.tb01965.x
30. C.S. Kim, S.H. Choi, J.K. Chai et al., J. Periodontol. **75**, 229 (2004). doi:10.1902/jop.2004.75.2.229
31. C.S. Kim, S.H. Choi, K.S. Cho et al., J. Clin. Periodontol. **32**, 583 (2005). doi:10.1111/j.1600-051X.2005.00729.x
32. Y.J. Yeo, D.W. Jeon, C.S. Kim et al., J. Biomed. Mater. Res. B Appl. Biomater. **72**, 86 (2005). doi:10.1002/jbm.b.30121
33. S.N. Bhaskar, J.M. Brady, L. Getter et al., Oral. Surg. Oral. Med. Oral. Pathol. **32**, 336 (1971). doi:10.1016/0030-4220(71)90238-6
34. P. Weiss, P. Layrolle, L.P. Clergeau et al., Biomaterials **28**, 3295 (2007). doi:10.1016/j.biomaterials.2007.04.006
35. G. Daculsi, R.Z. LeGeros, C. Deudon, Osseo-coalescence versus osseo-integration. Scanning Microscopy **4**, 309 (1990)
36. H. Yuan, Z. Yang, J.D. De Bruij, K. De Groot, X. Zhang, Biomaterials **22**, 2617 (2001). doi:10.1016/S0142-9612(00)00450-6
37. L.L. Hench, Science **208**, 826 (1980). doi:10.1126/science.6246576
38. N.M. Farina, F.M. Guzon, M.L. Pena, A.G. Cantalapiedra, J. Mater. Sci. Mater. Med. **19**, 1565 (2008). doi:10.1007/s10856-008-3400-y
39. H. Yuan, Z. Yang, Y. Li, X. Zhang, J.D. De Bruijn, K. De Groot, J. Mater. Sci. Mater. Med. **9**, 723 (1998). doi:10.1023/A:1008950902047
40. H. Yuan, K. Kurashina, J.D. de Bruijn, Y. Li, K. de Groot, X. Zhang, Biomaterials **20**, 1799 (1999). doi:10.1016/S0142-9612(99)00075-7
41. H. Yuan, J.D. De Bruijn, Y. Li, J. Feng, Z. Yang, K. De Groot et al., J. Mater. Sci. Mater. Med. **12**, 7 (2001). doi:10.1023/A:1026792615665
42. U. Ripamonti, Biomaterials **17**, 31 (1996). doi:10.1016/0142-9612(96)80752-6
43. N. Kawai, S. Niwa, M. Sato, Y. Sato, Y. Suwa, I. Ichihara, J. Biomed. Mater. Res. **37**, 1 (1997). doi:10.1002/(SICI)1097-4636(199710)37:1<1::AID-JBM1>3.0.CO;2-W
44. E. Tsuruga, H. Takita, H. Itoh, Y. Wakisaka, Y. Kyboki, J. Biochem. **121**, 317 (1997)
45. D. Olton, J. Li, M.E. Wilson, T. Rogers, J. Close, L. Huang et al., Biomaterials **28**, 1267 (2007). doi:10.1016/j.biomaterials.2006.10.026
46. M.A.W. Merkx, J.C. Matthias, M. Hans-Peter, Biomaterials **20**, 2029 (1999). doi:10.1016/S0142-9612(99)00105-2
47. U.M. Wikesjo, P. Guglielmoni, A. Promsudthi et al., J. Clin. Periodontol. **26**, 392 (1999). doi:10.1034/j.1600-051X.1999.260610.x
48. H.Y. Kim, C.S. Kim, G.J. Jhon et al., J. Peridontol. **73**, 1457 (2002). doi:10.1902/jop.2002.73.12.1457
49. J.S. Park, S.H. Choi, I.S. Moon et al., J. Clin. Peridontol. **30**, 443 (2003). doi:10.1034/j.1600-051X.2003.10283.x
50. S.H. Choi, C.K. Kim, K.S. Cho et al., J. Peridontol. **73**, 63 (2002)